CMI

www.nature.com/cmi

ARTICLE

A triple-RBD-based mucosal vaccine provides broad protection against SARS-CoV-2 variants of concern

Jingyi Yang[1,7], Mei-Qin Liu[2,3,7], Lin Liu[4,7], Xian Li[1,2,3], Mengxin Xu[4], Haofeng Lin[2,3], Shuning Liu[4], Yunqi Hu[4], Bei Li[2], Bowen Liu[2,3], Min Li[1], Ying Sun[5], Yao-Qing Chen[4,6]✉, Zheng-Li Shi[2]✉ and Huimin Yan[1]✉

© The Author(s), under exclusive licence to CSI and USTC 2022

The rapid mutation and spread of SARS-CoV-2 variants urge the development of effective mucosal vaccines to provide broad-spectrum protection against the initial infection and thereby curb the transmission potential. Here, we designed a chimeric triple-RBD immunogen, 3Ro-NC, harboring one Delta RBD and two Omicron RBDs within a novel protein scaffold. 3Ro-NC elicits potent and broad RBD-specific neutralizing immunity against SARS-CoV-2 variants of concern. Notably, intranasal immunization with 3Ro-NC plus the mucosal adjuvant KFD (3Ro-NC + KFDi.n) elicits coordinated mucosal IgA and higher neutralizing antibody specificity (closer antigenic distance) against the Omicron variant. In Omicron-challenged human ACE2 transgenic mice, 3Ro-NC + KFDi.n immunization significantly reduces the tissue pathology in the lung and lowers the viral RNA copy numbers in both the lung (85.7-fold) and the nasal turbinate (13.6-fold). Nasal virologic control is highly correlated with RBD-specific secretory IgA antibodies. Our data show that 3Ro-NC plus KFD is a promising mucosal vaccine candidate for protection against SARS-CoV-2 Omicron infection, pathology and transmission potential.

Keywords: SARS-CoV-2; Mucosal vaccine; Intranasal immunization; Triple-RBD; Flagellin adjuvant; Variant of concern

Cellular & Molecular Immunology (2022) 19:1279–1289; https://doi.org/10.1038/s41423-022-00929-3

INTRODUCTION

The worldwide COVID-19 pandemic has lasted for more than 2 years since early 2020. New infections are still escalating periodically around the world although many COVID-19 vaccines have been developed. Several different vaccines have been clinically deployed globally. It is evident that the pandemic has not been efficiently impeded either by current mass vaccination or by enforcement of moderate nonpharmaceutical interventions and stringent border control measures, such as those performed by Hong Kong [1] and even by North Korea. In the past 2 years, the Alpha (B.1.1.7), Beta (B.1.351), Gamma (P.1), and Delta (B.1.617.2) lineages have arisen successively in different countries and have raised serious questions about the nature, extent, and consequences of antigenic drift in SARS-CoV-2. In particular, the latest emergent Omicron (B.1.1.529) lineage, which was initially isolated in South Africa and harbors more than 30 mutations in the spike protein, has become prominent worldwide [2]. The unpredicted emergence of antigenically distinct SARS-CoV-2 variants of concern (VOCs) has increased the risk of disease spread globally and has resulted in COVID-19 pandemic waves.

According to clinical findings [3], SARS-CoV-2 infection and replication usually start in the nasal ciliated cells, where serum IgG is rarely accessible. Thus, current vaccines aimed at COVID-19 mostly avert syndromes but not contagion, especially the initial viral entry into and infection of the upper respiratory tract. The highly transmissible variant of Omicron is vaccine evasive and causes breakthrough infections. Furthermore, more than 90% of the Omicron infections are asymptomatic or mild cases, but such individuals harbor replicating SARS-CoV-2 in their nasopharyngeal mucosa and can communicate it to others [2, 4]. Therefore, the current intramuscularly injected COVID-19 vaccines could hardly end the pandemic. Hence, it is urgent to explore an effective mucosal vaccine that can prevent the infection and transmission of SARS-CoV-2 variants.

The spike protein on the SARS-CoV-2 virus surface mediates viral attachment and entry via the receptor-binding domain (RBD) regions, which makes it a potential target for COVID-19 vaccine design [5, 6]. RBD-based antigens have been widely used in coronavirus vaccine development [7]. To date, approximately 15 RBD-based vaccines for COVID-19 are under development at different stages [8]. However, SARS-CoV-2 vaccine protection rates decline as COVID-19 mutants emerge, especially those with RBD mutations. To overcome the limited immunogenicity of the viral RBD antigen and induce a broad-spectrum immune response, chimeric RBD-dimer immunogen strategies have been designed via tandem RBDs of different strains [9]. The SARS-CoV-2 RBD

[1]Vaccine and Immunology Research Center, Translational Medical Research Institute, Shanghai Public Health Clinical Center, Fudan University, 201508 Shanghai, China. [2]Wuhan Institute of Virology, Chinese Academy of Sciences, 430071 Wuhan, China. [3]University of Chinese Academy of Sciences, 100049 Beijing, China. [4]School of Public Health (Shenzhen), Shenzhen Campus of Sun Yat-sen University, Shenzhen 518107 Guangdong, China. [5]Aerosol Bio-Tech (Suzhou) Co., LTD, Suzhou 215123 Jiangsu, China. [6]Key Laboratory of Tropical Disease Control (Sun Yat-sen University), Ministry of Education, Guangzhou, China. [7]These authors contributed equally: Jingyi Yang, Mei-Qin Liu, Lin Liu. ✉email: chenyaoqing@mail.sysu.edu.cn; zlshi@wh.iov.cn; yanhuimin@shphc.org.cn

Received: 15 July 2022 Accepted: 12 September 2022
Published online: 11 October 2022

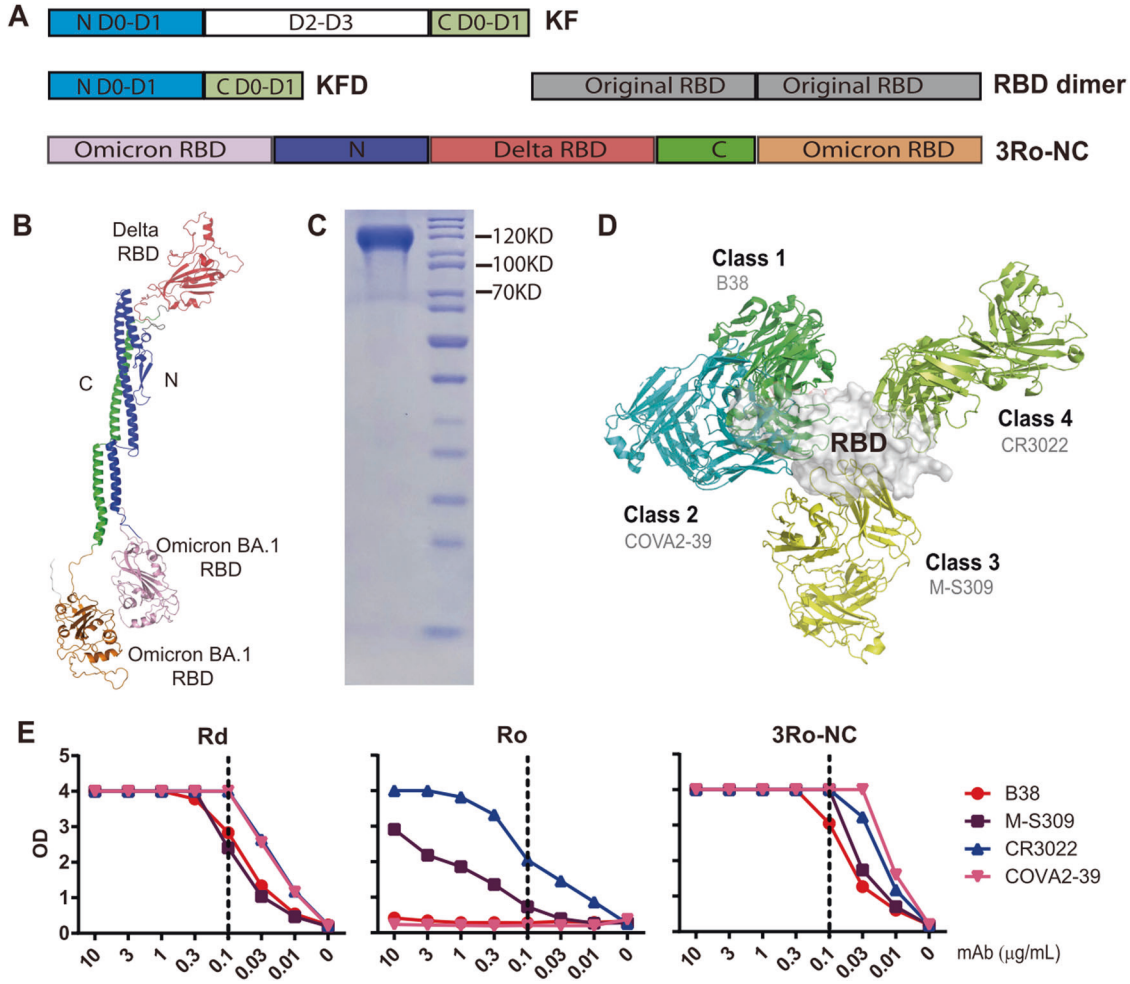

Fig. 1 Construction of the chimeric triple-RBD protein 3Ro-NC. **A** Schematic diagram of flagellin KF, KFD and chimeric protein 3Ro-NC. KFD was derived from the D0 and D1 domains of flagellin KF. The scaffold NC was designed based on the 3D structure of KFD. One *RBD* gene of the SARS-CoV-2 Delta strain and two *RBD* genes of the Omicron BA.1 strain were connected by the *NC* gene to generate the *3Ro-NC* gene. **B** 3D structure of the protein 3Ro-NC predicted by Alpha Fold 2. **C** SDS–PAGE analysis of the purified protein 3Ro-NC. **D** Diagram of the binding of the SARS-CoV-2 RBD with four classes of neutralizing mAbs. **E** Binding ability of the Delta strain RBD (Rd), Omicron BA.1 strain RBD (Ro) and 3Ro-NC with the four classes of representative neutralizing mAbs analyzed by ELISA. The data shown represent one of three independent experiments, each with duplicates

conjugated with the Fc fragment of human IgG, as an immunopotentiator, can elicit robust antibody neutralizing activity against SARS-CoV-2 infections in mice [10]. However, the current RBD-based subunit vaccines do not strongly induce mucosal immune responses in the respiratory tract that can prevent SARS-CoV-2 nasal infection and asymptomatic transmission.

To address this problem, we designed and tested the chimeric triple-RBD immunogen 3Ro-NC, which contains one delta RBD and two RBDs of Omicron subvariant BA.1 within a new scaffold NC, to investigate whether it can be used for mucosal vaccination to inhibit SARS-CoV-2 variants from spreading infection. We once developed a kind of recombinant flagellin KFD as a mucosal adjuvant, which was proven to be safe and effective for intranasal immunization in our previous works [11, 12]. KFD exerts its immune modulating activity by activating the TLR5 pathway in nasal epithelial cells and enhancing local and distal mucosal IgA responses [13, 14]. In this study, the immunogenicity of 3Ro-NC was assessed by intramuscular injection with an aluminum adjuvant (AL-adjuvant) or by intranasal vaccination with a recombinant flagellin protein KFD adjuvant (KFD). Here, we show that intranasal immunization of 3Ro-NC adjuvanted with KFD elicits broad-spectrum immune responses as well as potent mucosal immune responses, particularly mucosal IgA antibody responses in the upper respiratory tract. The immune responses confer protection against viral infection in the upper and lower respiratory tract in mice.

RESULTS

A chimeric triple-RBD protein 3Ro-NC preserves neutralizing epitopes

A truncated *E. coli* K12 strain flagellin KF, named KFD, containing the D0 and D1 domains, was constructed as previously reported [12, 15]. The scaffold N-terminal domain (N) and C-terminal domain (C) were designed based on the 3D structure of KFD. One copy of the RBD of the SARS-CoV-2 Delta strain and two copies of the RBD of Omicron subvariant BA.1 were connected by the N and C to generate a recombinant RBD construct, named 3Ro-NC (Fig. 1A, B).

The immunogen 3Ro-NC was expressed in 293F cells and purified as a single band with a molecular mass of ~120 kDa (Fig. 1C). In contrast to the *E. coli* system expressing the flagellin fusion protein P-KFD1 that we generated previously [11], protein 3Ro-NC has no toll-like receptor 5 (TLR5)-stimulating activity (Fig. S1). Four monoclonal antibodies (mAbs), B38, M-S309, CR3022 and COVA2-39, which represent four classes of RBD-specific neutralizing antibodies [16] (Fig. 1D), were then chosen to

test the reactivity and conformation of the RBDs on 3Ro-NC. As shown in Fig. 1E, while the monomeric RBD of the Delta variant (Rd) showed potent binding ability with all four mAbs, the monomeric RBD of Omicron variant BA.1 (Ro) had significantly diminished binding ability with mAb CR3022 and M-S309 and eliminated binding ability with B38 and COVA2-39. In contrast, 3Ro-NC had a high binding ability with all four mAbs and even significantly higher affinities than Rd. These results indicate that at least the Delta RBD epitopes in 3Ro-NC retain the native conformation structure.

3Ro-NC elicits broad and potent neutralizing antibodies against SARS-CoV-2 variants, including Omicron

To analyze the immunogenicity of 3Ro-NC, BALB/c mice were intramuscularly immunized three times with a 4 μg/dose of the 3Ro-NC or an RBD dimer of the original strain [9] with aluminum adjuvant (AL-adjuvant). Saline alone was given as a control. Mouse serum samples were collected at 14 days after each immunization (Fig. 2A), and ELISA was used to measure humoral responses. After the 1st and 2nd immunizations, the 3Ro-NC elicited considerably greater RBD-specific IgG responses against not only the RBD of Omicron BA.1 and Delta variants but also the RBD of Gamma and the original strain of SARS-CoV-2 compared to the RBD dimer (Fig. 2B). Notably, only the 3Ro-NC induced a prominent Omicron RBD-specific IgG response after the 1st immunization.

The neutralizing antibodies against SARS-CoV-2 VOCs were assessed by a pseudotyped viral assay. After the 2nd and 3rd immunizations, sera from the 3Ro-NC-immunized mice potently neutralized all tested SARS-CoV-2 variant pseudotyped viruses (Fig. 2C) and even the SARS-CoV-1 pseudotyped virus (Fig. 2D). Moreover, although not significant at all time points, the neutralizing titers induced by 3Ro-NC were higher than those induced by the RBD dimer, especially against the most prevalent Omicron variants BA.1, BA.2, BA.4 and BA.5. Notably, only 3Ro-NC induced prominent neutralizing antibodies against Omicron BA.1 and the original strains after the 1st immunization (Fig. 2E). The geometric mean titer of neutralizing antibodies also revealed that 3Ro-NC could induce potent neutralizing antibody responses against all the tested SARS-CoV-2 variants as well as SARS-CoV-1 (Fig. 2F). More importantly, the neutralization titer ratios of the Omicron variant BA.1 to the original strain, as well as to the Delta variant, in the 3Ro-NC-immunized mice were significantly higher than those in the RBD dimer-immunized mice (6.1-fold and 10.7-fold, respectively, after the 3rd immunization) (Fig. 2G). This suggests that antibody responses elicited by 3Ro-NC can readily neutralize Omicron, which has the potential to evade the neutralization activity elicited by previous SARS-CoV-2 VOCs.

We also applied antigenic cartography to explore how the serum samples distinguish the different spike antigens [17]. Antigenic maps were made separately using the neutralizing antibody titers after the 2nd or 3rd immunization (Fig. 2H). For the RBD dimer group, the serum samples after the 2nd and 3rd vaccinations (Fig. 2H upper panels) were more tightly clustered around the original and Delta strains. In agreement with the neutralizing titers (Fig. 2C, E, F, G), the antigenic distances between Omicron BA.1 and the original or Delta strain were large for these two sets of RBD dimer-immunized sera. For the 3Ro-NC group, although the serum samples after the 2nd vaccination were still tightly clustered around the original and Delta strains, the antigenic distance between Omicron BA.1 and the original strain (9.2-fold difference) was closer than that of the RBD dimer group (25.1-fold difference) (Fig. 2H left panels). After the 3rd vaccination with 3Ro-NC, the distances between Omicron BA.1 and Delta were markedly reduced from a 26.9-fold difference to a 3.5-fold difference (Fig. 2H lower panels). More remarkably, after the 3rd vaccination, the antigenic distance between Omicron BA.1 and the original or Delta in the 3Ro-NC group (6.1- and 3.5-fold difference, respectively) was much closer than that in the RBD dimer group (55.7- and 48.5-fold difference, respectively) (Fig. 2H right panels). The change in antigenic distance to Omicron BA.1 suggests that the increase in the proportion of neutralizing antibodies against Omicron BA.1 occurs after the 3rd immunization in the 3Ro-NC. These results indicate that 3Ro-NC induces potent and broad RBD-specific IgG responses against SARS-CoV-2 variants and even SARS-CoV-1. The results also suggest that the combination of different RBDs, such as Omicron plus Delta, with the NC scaffold is a promising antigen design strategy for integrating multiple RBDs to elicit potent and broad RBD-specific IgG responses.

Intranasal immunization with KFD-adjuvanted 3Ro-NC elicits coordinated systemic and mucosal immunity against the Omicron variant

A suitable mucosal adjuvant is essential for a subunit protein immunogen in developing an effective mucosal vaccine. Flagellin-derived recombinant protein KFD was chosen as a mucosal adjuvant to test 3Ro-NC as a mucosal immunogen as previously reported [11, 13–15]. Briefly, BALB/c mice were intranasally immunized with 4 μg 3Ro-NC plus 1 μg KFD adjuvant (*3Ro-NC + KFDi.n*) or intramuscularly immunized with 4 μg 3Ro-NC plus 200 μg AL-adjuvant (*3Ro-NC + ALi.m*) 3 times. Saline alone was given as a control. Mouse serum and mucosal samples were collected at 14 days after each immunization, and ELISA was used to measure the humoral responses (Fig. 3A). The results showed that group immunization with *3Ro-NC + KFDi.n* induced similar levels of RBD-specific IgG responses to those in the group administered *3Ro-NC + ALi.m* after the 2nd and 3rd immunizations, although much lower antibody titers were observed in the *3Ro-NC + KFDi.n* group after the 1st immunization (Fig. 3B and Fig. S2).

Serum neutralizing antibodies were also assessed with pseudotyped viruses. In general, the sera from the *3Ro-NC + KFDi.n*-immunized mice after the 2nd and 3rd immunizations potently neutralized all the tested SARS-CoV-2 variants and even SARS-CoV-1, although with slightly lower neutralizing titers than those from *3Ro-NC + ALi.m*-immunized mice for most variants (Fig. 3C, D). It is interesting that the geometric mean neutralizing titers (GMT) against Omicron BA.1 in the sera of *3Ro-NC + KFDi.n*-immunized mice were even higher than those in *3Ro-NC + ALi.m*-immunized mice, especially at the time point after the 2nd immunization (Fig. 3D). It should be noted that only in the *3Ro-NC + KFDi.n*-immunized group, neutralizing antibody titers against the Omicron variant BA.1 were comparable with those the Delta variant, and even higher than those against the original strain (Fig. 3C, D). This tendency was more prominent at the time point after the 2nd immunization than at the timepoint after the 3rd immunization (Fig. 3E). Accordingly, in the *3Ro-NC + KFDi.n*-immunized mice, ratio of the neutralization titers against the Omicron variant BA.1 to those against the original strain, as well as to those against the Delta variant, were significantly higher than those in the *3Ro-NC + ALi.m*-immunized mice (42-fold and 32-fold, respectively, after the 2nd immunization) (Fig. 3E).

We also applied antigenic cartography to explore how the sera of 3Ro-NC intranasally immunized mice distinguish different spike antigens [17]. Antigenic maps were made separately or together using the neutralizing antibody titers after the 2nd or 3rd immunization (Fig. 3F, G). For the *3Ro-NC + KFDi.n* group, the serum samples after the 2nd and 3rd vaccinations were all tightly clustered around the Delta and Omicron BA.1 strains (Fig. 3F, G), while the serum samples of the *3Ro-NC + ALi.m* group were all tightly clustered around the Delta strains (Fig. 2H lower panels and Fig. 3G). After the 2nd vaccination, the antigenic distance between Omicron BA.1 and Delta in the *3Ro-NC + KFDi.n* group (6.1-fold difference) was closer than that in the *3Ro-NC + ALi.m* group (26.9-fold difference) (Fig. 3F left panel and Fig. 2H left lower panel). After the 3rd vaccination, the antigenic distance between Omicron BA.1 and the original or Delta strain in the *3Ro-NC + KFDi.n* group (2.8-

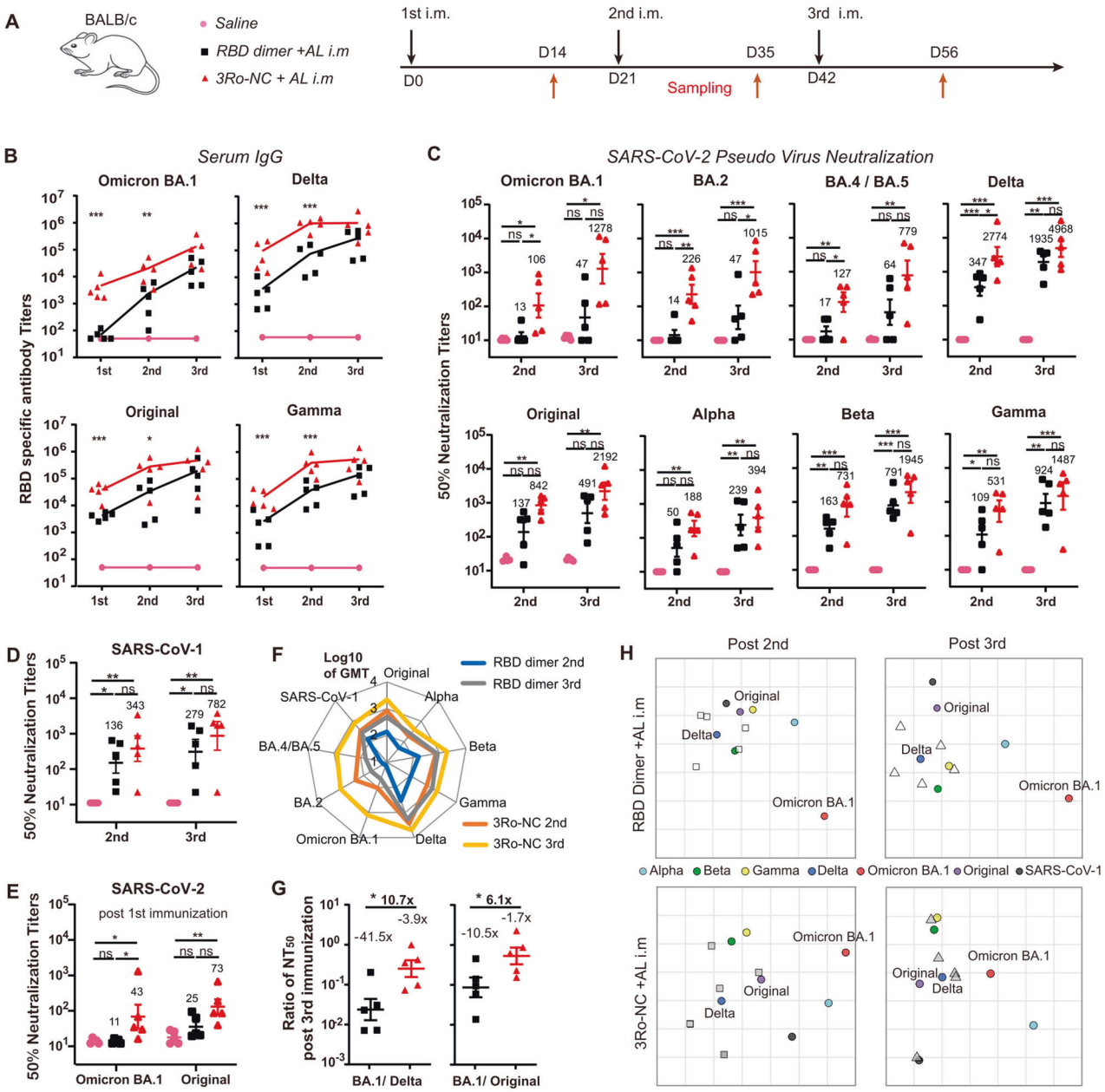

Fig. 2 Immunogenicity of 3Ro-NC in the presence of aluminum adjuvant in BALB/c mice. **A** Diagrammatic scheme of the immunization and sampling ($n = 5$ mice per group). **B** RBD-specific IgG responses in serum. **C**–**H** Neutralizing antibody responses in serum tested in a pseudotyped virus system. Neutralizing antibody titers after the 2nd and 3rd immunizations against pseudotyped SARS-CoV-2 variants (**C**) or SARS-CoV-1 (**D**). **E** Neutralizing antibody titers against SARS-CoV-2 Omicron BA.1 and the original strain after the 1st immunization. **F** Geometric mean titers (GMT) of neutralizing antibodies against different variants. **G** The ratios of neutralizing antibody titer (the 50% neutralizing titer, NT_{50}) against Omicron BA.1 to that against the original strain or Delta. **H** Antigenic maps were generated from the second (square) or third vaccination (triangle) serum samples of RBD dimer (white) and 3Ro-NC (gray) groups. Cyan, green, yellow, blue, red, purple, and black circles correspond to the Alpha, Beta, Gamma, Delta, Omicron BA.1, original strains and SARS-CoV-1, respectively. Each grid square corresponds to a twofold dilution in the neutralization assay. The antigenic distance is interpretable in any direction. Data are represented as the mean ± SEM and are representative of at least two independent experiments. In (**B**) and (**G**), two immunized groups were compared using an unpaired *t*-test. In (**C**–**E**), groups were compared using one-way ANOVA. $^{*}P < 0.05$; $^{**}P < 0.01$; $^{***}P < 0.001$; ns, nonsignificant; GMT of NT_{50} are indicated

and 1.7-fold difference, respectively) was still closer than that in the *3Ro-NC + ALi.m* group (6.1- and 3.5-fold difference, respectively) (Fig. 3F right panel and Fig. 2H right lower panel). The differences in antigenic distance to Omicron BA.1 reflect the finding that compared to 3Ro-NC + ALi.m immunization, *3Ro-NC + KFDi.n* immunization has a tendency to induce stronger antibody responses to neutralize Omicron variant BA.1. These results indicate that the change in immunization route and adjuvant type apparently alters the specificity of antibody responses.

Next, we focused on the evaluation of mucosal immune responses. As expected, only intranasal immunization (*3Ro-NC + KFDi.n*) elicited significant RBD-specific mucosal IgA antibody responses against both Omicron BA.1 and Delta RBDs in saliva (Fig. 3H). In addition, similar IgA levels of responses were detected in vaginal lavage fluid (Fig. 3I) and nasal lavage fluid (Fig. 3J right panel) after the 3rd intranasal immunization. A high correlation between RBD-specific IgA titers in nasal lavage fluid and saliva was observed (Fig. S3A), indicating that salivary IgA responses can

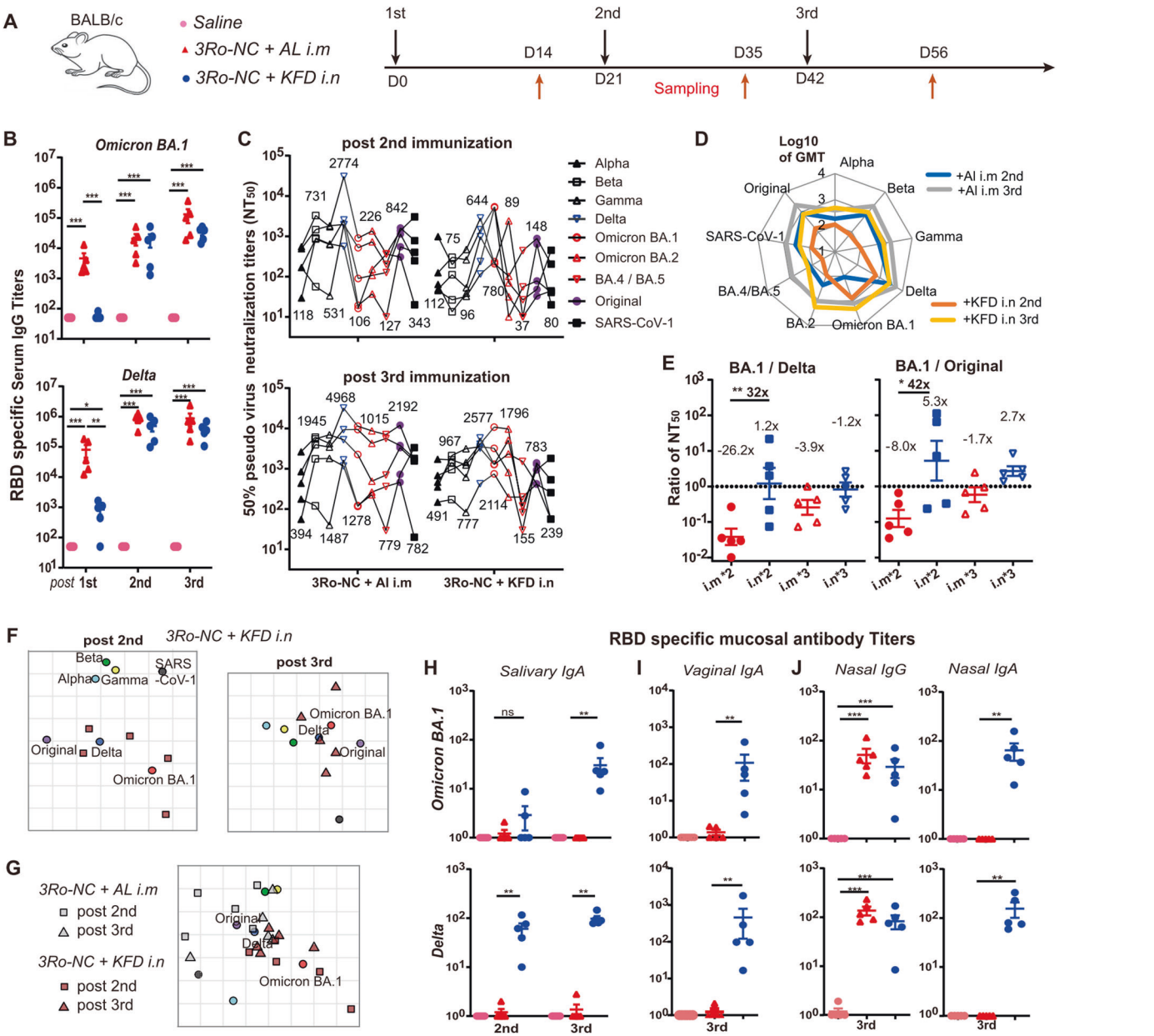

Fig. 3 Antibody responses by the intranasal immunization of 3Ro-NC adjuvanted with KFD in BALB/c mice. **A** Diagrammatic scheme of the immunization and sampling ($n = 5$ mice per group). **B** RBD-specific IgG responses in serum. **C**–**G** Neutralization antibody responses in serum tested in a pseudotyped virus system. **C** Neutralization antibody titers against the pseudotyped SARS-CoV-2 variants or SARS-CoV-1 in serum after the 2nd and 3rd immunizations. Each connecting line indicates the neutralizing titers of one individual serum sample against different virus strains. **D** Geometric mean titers of the neutralizing antibodies in serum against different variants. **E** The ratio of neutralizing antibody titers against Omicron BA.1 to those against Delta or the original strain. **F**, **G** Antigenic maps were generated from the second (square) or the third vaccination (triangle) serum samples of the *3Ro-NC + KFDi.n.* group (brown) and *3Ro-NC + ALi.m.* group (gray). Cyan, green, yellow, blue, red, purple, and black circles correspond to the Alpha, Beta, Gamma, Delta, Omicron BA.1, original strain and SARS-CoV-1, respectively. Each grid square corresponds to a twofold dilution in the neutralization assay. The antigenic distance is interpretable in any direction. **H**–**J** RBD-specific mucosal IgA responses in saliva (**H**), vaginal lavage fluid (**I**) and nasal turbinate lavage fluid (**J**). Data are presented as the mean ± SEM and are representative of at least two independent experiments.; GMT of NT_{50} are indicated. Groups were compared using one-way ANOVA. $^*P < 0.05$; $^{**}P < 0.01$; $^{***}P < 0.001$; ns, nonsignificant

reflect the IgA response in the upper respiratory tract. When comparing different vaccination routes, similar titers of RBD-specific IgG (~10^2) could be detected in the nasal cavity lavage fluid in both the intramuscularly (*3Ro-NC + KFDi.m*) and intranasally (*3Ro-NC + KFDi.n*) immunized mice (Fig. 3J left panel). This detectable lower titer of RBD-specific mucosal IgG showed a high correlation with the high titer of RBD-specific serum IgG (Fig. S3B).

Collectively, these results showed that 3Ro-NC adjuvanted with KFD is highly immunogenic by intranasal immunization, which can elicit coordinated systemic and local mucosal immune responses against different SARS-CoV-2 variants, especially Omicron.

The coordinated mucosal and systemic immunity protects mice from Omicron infection and pathology

To further explore the protective efficacy of the 3Ro-NC vaccine, human ACE2 transgenic mice (hACE2) were utilized to evaluate the mucosal protection against SARS-CoV-2 Omicron variant BA.1 infection. In brief, mice were immunized with 4 μg of 3Ro-NC plus

1 μg KFD via the intranasal route (*3Ro-NC + KFDi.n.)*, 3Ro-NC plus AL-adjuvant via the intramuscular route (*3Ro-NC + ALi.m.)*, or 2.5 μg inactivated SARS-CoV-2 with 200 μg AL-adjuvant via the intramuscular route (*IAV + ALi.m.)*, using saline inoculation as the control group (Fig. 4A).

In line with the results in BALB/c mice, robust serum IgG antibody responses against Omicron BA.1, Delta (Fig. 4B) and Gamma RBD (Fig. S4) were induced in the mice by intranasal immunization of 3Ro-NC plus KFD, intramuscular immunization of 3Ro-NC plus AL, and IAV plus AL. The group receiving *IAV + ALi.m* generated the lowest RBD specific serum IgG, while the group receiving *3Ro-NC + KFDi.n* developed the highest Omicron RBD specific serum IgG (Fig. 4B). However, RBD-specific IgA in the saliva and vaginal lavage fluid (Fig. 4B) could only be induced in the mice of the *3Ro-NC + KFDi.n* group. The neutralizing antibodies against SARS-CoV-2 Omicron in serum after the 3rd immunization were assessed by using authentic SARS-CoV-2 Omicron BA.1. Sera from the *3Ro-NC + KFDi.n*-immunized mice showed much higher neutralizing antibody titers (NT_{50}) against SARS-CoV-2 Omicron BA.1 than did the sera either from the *IAV + ALi.m*-immunized mice or from the *3Ro-NC + KFDi.m*-immunized mice (Fig. 4C). The neutralizing activities (NT_{50}) against SARS-CoV-2 Omicron BA.1 were significantly correlated with the titers of Omicron BA.1 RBD-specific serum IgG (Fig. 4D).

At 28 days after the 3rd immunization, the mice were intranasally challenged with 5×10^4 $TCID_{50}$ Omicron BA.1 in 50 μl. Three days post-infection, viral loads in the lungs and nasal turbinate tissues were determined using qPCR and plaque assays. In the lung tissue, viral genome copy numbers were significantly reduced in both the *IAV + ALi.m* group and the *3Ro-NC + KFDi.n* group by 82.2-fold and 85.7-fold, respectively, compared to the PBS control group (Fig. 4E, left panel). In the *3Ro-NC + ALi.m* group, only some mice showed a reduced Omicron viral load in lung tissue (Fig. 4E), although the Omicron BA.1 RBD-specific serum IgG titers and neutralizing titers in this group were even higher than those in the *IAV + ALi.m* group (Fig. 4B, C). Infectious virus could hardly be detected by plaque assay in the lung tissues of all three immunized groups except for one mouse in the *3Ro-NC + ALi.m* group, in contrast to that in the saline control group (Fig. 4E, right panel). The disparity of the high viral load but low PFU detected in lung tissue may have resulted from the much lower replication efficacy of the omicron strain BA.1 in hACE2 mice and in the assay using Vero E6 cells.

Meanwhile, a histopathological examination was performed to analyze infection- and immunization-related inflammation in the lungs after virus challenge (Fig. 4F). In all four challenged groups, no severe pathology in the lung was observed (Fig. 4G). To our surprise, while thickened alveolar walls, edema and fibrosis were occasionally observed, widely distributed inflammatory cell infiltration could be seen in the lungs of IAV-immunized mice, especially around perivascular sites (Fig. 4H). In contrast, inflammatory cell infiltration was apparently reduced in the lungs of mice immunized with *3Ro-NC + KFDi.n*. Notably, only the *3Ro-NC + KFDi.n* group showed a substantial viral decrease in the nasal turbinates, compared to either the saline group (13.6-fold) or the other two intramuscularly immunized *IAV + ALi.m* groups (8.4-fold) and *3Ro-NC + KFDi.m* group (10.7-fold) (Fig. 4I). These results indicate that intranasal immunization with 3Ro-NC plus KFD adjuvant can restrict infection and pathology in the airway and lung, suggesting that 3Ro-NC plus KFD can provide protection against Omicron infection in both upper- and lower- respiratory tracts as a prophylactic mucosal SARS-CoV-2 vaccine.

In all vaccinated groups, the protection from infection of the turbinates (Fig. 4I) was only observed in mice that received intranasal immunization, which generated both protective serum IgG and mucosal IgA. This triggered the question of whether mucosal IgA and IgG exert different protective effects in the upper and lower respiratory tracts. Accordingly, in our experiments, no significant correlation of viral copy numbers between lung tissue and turbinates could be observed (Fig. 4J). Due to the lack of a nasal cavity obtained before scarification of the mice, we selected salivary IgA and serum IgG, which were highly correlated with the levels of nasal IgA and IgG, respectively (Fig. S3), as representatives of humoral immune responses. In lung tissue, the viral RNA copy number was negatively correlated with the serum IgG titer but not with the salivary IgA titer (Fig. 4K). On the other hand, the viral RNA copy numbers in the nasal turbinate tissue were only negatively correlated with salivary IgA titers but not serum IgG titers (Fig. 4L). These results indicate that protection of the lung and turbinate was mainly provided by RBD-specific IgG responses and mucosal IgA, respectively.

DISCUSSION

Here, we developed a new chimeric triple-RBD protein, 3Ro-NC, which harbors one copy of the Delta RBD and two copies of the Omicron BA.1 RBD in a single recombinant protein. Intramuscular immunization of 3Ro-NC with adjuvant aluminum induces a broad-spectrum IgG response against homogenous Delta and Omicron RBDs as well as heterogeneous Gamma and the prototype original strain RBDs detected by ELISA and pseudotyped viral neutralization assays. Intranasal immunization of 3Ro-NC with the recombinant flagellin protein KFD [12, 15] promotes a stronger immune response than intramuscular immunization of 3Ro-NC with the aluminum adjuvant. Our data demonstrated that 3Ro-NC adjuvanted with KFD is highly immunogenic by intranasal immunization, which can elicit coordinated systemic and local mucosal immune responses against different SARS-CoV-2 variants, especially Omicron BA.1. The coordinated mucosal and systemic immunity induced by intranasal immunization with 3Ro-NC plus KFD significantly decreased the viral load in the lung and especially in the nasal turbinate tissue after nasal challenge with SARS-CoV-2 Omicron BA.1 in the hACE2 transgenic mouse model. The viral load in the nasal turbinate is reversely correlated with the mucosal IgA titer in saliva.

In the past 2 years of the COVID-19 pandemic, unprecedented development of an effective SARS-CoV-2 vaccine has been achieved by utilizing novel mRNA vaccine technology as well as by traditional inactivated vaccine or replication-deficient adenoviral vector methodologies. Unfortunately, these presently permitted SARS-CoV-2 vaccines are mostly administered parenterally and induce little mucosal immunity in the respiratory tract; thus, they have been proven only effective in preventing individual morbidity and mortality but not as efficient in preventing infection and transmission. Furthermore, the frequent emergence of SARS-CoV-2 VOCs throughout the pandemic has highlighted the urgent need for effective mucosal vaccines that not only protect the individual from severe disease but also prevent viral infection and transmission. Our data demonstrated that 3Ro-NC plus KFD as a subunit mucosal vaccine significantly reduced the viral load in both the nasal cavity and the lung compared to the parenteral administration strategy, indicating promising potential of the new chimeric protein 3Ro-NC in reducing infection and transmission, especially for curbing the current Omicron pandemic.

Mucosal vaccines, which can trigger robust protective immune responses at the local sites of pathogen infection, have become increasingly recognized due to their capacity to prevent an infection from becoming established in the very initial site rather than only curtailing infection and disease symptoms [18]. In line with this concept, at least seven intranasal SARS-CoV-2 vaccine candidates are in ongoing clinical trials worldwide. Most recently, the safety and immunogenicity of a live attenuated influenza virus vector-based intranasal SARS-CoV-2 vaccine, dNS1-RBD, in adults were reported [19]. While this needle-free intranasal vaccine was well tolerated in adults, only weak humoral and mucosal immune responses against SARS-CoV-2 were detected in vaccine recipients.

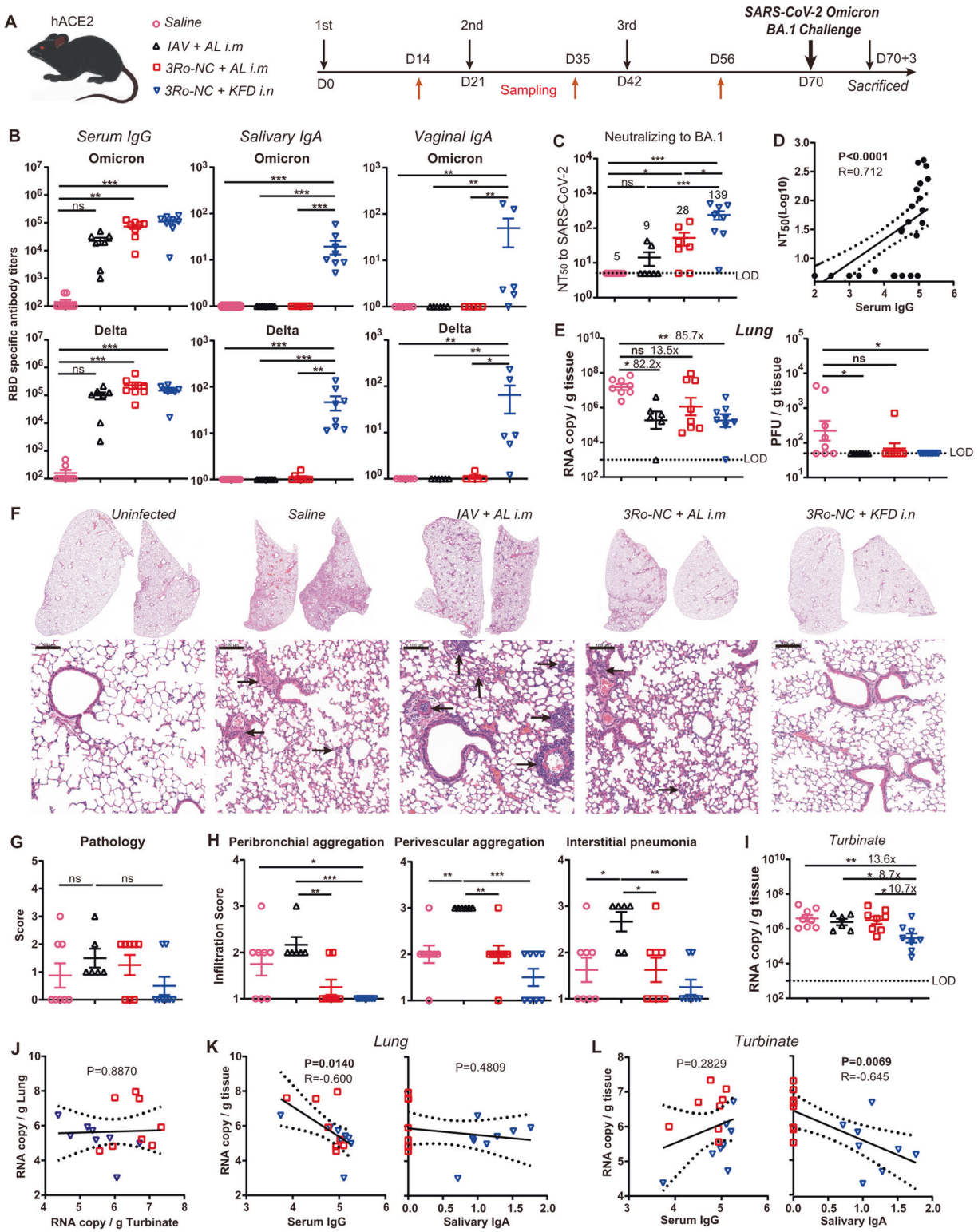

Fig. 4 Protection of 3Ro-NC-immunized hACE2 mice against SARS-CoV-2 variant Omicron infection. **A** Diagrammatic scheme of the immunization and virus challenge ($n = 6–8$ mice per group). **B** RBD-specific serum IgG, salivary IgA and vaginal IgA after the 3rd immunization. **C** Neutralization antibody titers against authentic SARS-CoV-2 Omicron BA.1 in serum after the 3rd immunization. **D** Correlation of NT_{50} against Omicron BA.1 with the Omicron BA.1 RBD-specific serum IgG. **E** qPCR-tested RNA copies of SARS-CoV-2 RBD and plaque assay of infectious virus in the lung at 3 days post-infection. **F** Hematoxylin and eosin (H&E) staining of the lung sections (scale bars, 100 μm). Infiltrations of immunocytes are labeled by arrows. **G** Pathological scores according to the H&E-stained sections. **H** Infiltration score of immunocyte aggregation around bronchioles, pulmonary vessels and interstitial pneumonia. **I** qPCR was used to test RNA copies of SARS-CoV-2 RBD in turbinates at 3 days post-infection. **J** Correlation of RNA copies in the lung and turbinate. **K**, **L** Correlation of RNA copies in the lung and turbinate with Omicron BA.1 RBD-specific serum IgG and salivary IgA. The 95% confidence interval is indicated by dotted lines. Groups were compared using one-way ANOVA. $^{*}P < 0.05$; $^{**}P < 0.01$; $^{***}P < 0.001$; ns nonsignificant. LOD limit of detection

Regardless, the efficacy of this nasally administered vaccine needs to be confirmed by the results of an ongoing phase 3 trial. However, another clinical trial of an adenovirus-based intranasal SARS-CoV-2 vaccine, AdCOVID (Altimmune, Gaithersburg, MD, USA), was discontinued due to poor results from early clinical trials in June 2021. This again reminds us of a potential intrinsic shortcoming of viral vector-based vaccines for nasal immunization, in which the effect of preexisting anti-vector immunity likely impairs the efficacy of the vaccines, especially in translation from preclinical to clinical studies, due to distinct differences in preexisting immunity between experimental animals and humans. In this regard, subunit protein vaccines for nasal immunization may avert this problem because of the lack of associated preexisting immunity.

However, subunit protein vaccines for intranasal immunization face another challenge of their low immunogenicity and thus usually need the help of a mucosal adjuvant. As we previously developed a recombinant flagellin KFD and demonstrated it to be safe and effective for intranasal immunization [11, 12], in which KFD can activate the TLR5 pathway in nasal epithelial cells to enhance local and distal mucosal IgA responses [13, 14], we chose KFD as a mucosal adjuvant in the current study. Our results showed that 1 μg KFD facilitated a protective mucosal IgA response to 4 μg 3Ro-NC antigen protein, while robust systemic IgG antibody was also induced effectively. The reverse correlation between the viral RNA copy number in the nasal turbinate tissue and the IgA response in the saliva suggests the local mucosal IgA response's key role in protecting against initial viral entry and infection. We previously demonstrated that the flagellin truncated variant KFD has advantages over the full-length form and is more suitable as an adjuvant for vaccines [11, 12, 15]. The present study demonstrated again that KFD is an excellent mucosal adjuvant regarding its safety and effectivity profiles for the development of subunit vaccines [20].

On the other hand, the chimeric triple-RBD protein 3Ro-NC was screened and optimized for harboring more than one target RBD with a computationally designed protein scaffold NC. The recombinant protein is expressed productively in 293F cells and is heat-stable and immunogenic. Even one intramuscular injection of 3Ro-NC with aluminum adjuvant (AL-adjuvant) induced a high serum IgG antibody response in mice (Fig. 2), while the RBD dimer induced no detectable IgG response to the Omicron variant. A dimeric RBD containing one Omicron and one Delta RBD might be a better control for the comparison. However, our present results suggest that the combination of different RBDs with the NC scaffold is a promising antigen design strategy for integrating multiple RBDs. Our data also suggest that more than three RBDs might be harbored in one single protein that allows for the design of a multivalent subunit vaccine with more combinations of different RBDs other than just tandem links. If so, a broad-spectrum subunit mucosal vaccine might be constructed to address the shortcomings of current parenteral vaccines. A pan-cross-reacted mucosal IgA antibody induced by such vaccines might enhance protection against a more heterosubtypic VOC challenge via secretory IgA. The respiratory IgA response against multiple SARS-CoV-2 VOCs makes it possible to catch up with the frequent emergence of VOCs. The 3Ro-NC protein and KFD are soluble proteins that might be designed as a nasal spray vaccine for self-administration. This advantage will meet the urgent need for mass production and mass immunization for urgent use in the face of pandemics.

As several studies have reported, the virus persists longer in nasal swabs than in bronchoalveolar lavage following an Omicron challenge, which diverges from the findings from prior SARS-CoV-2 variants in macaques [21–23]. This suggests that the SARS-CoV-2 Omicron variant likely has a prolonged duration of virus shedding in the upper respiratory tract and a higher degree of transmissibility. Although we did not evaluate the duration of virus shedding in the upper respiratory tract directly in the mouse model, it is conceivable that intranasal immunization or a booster with 3Ro-NC should be able to decrease the transmissibility of the Omicron variant with the help of secretory respiratory IgA antibodies. On the other hand, a higher virus load was found to be associated with increased secondary transmission in household settings [24, 25]. In this regard, intranasal immunization with 3Ro-NC might likely lower the risk of secondary transmission to others even though breakthrough infection occurs in the immunized individual. Furthermore, a mucosally vaccinated individual may efficiently block early virus invasion because the initial virus amount is usually limited to a smaller number. Thus, hidden transmission by an asymptomatic individual might be blocked. Although our data showed that intranasal application of 3Ro-NC was not significantly superior to intramuscular injection at reducing viral replication in the lung and preventing pathology, intranasal immunization alone could significantly reduce the viral load in turbinates. These data provide evidence that intranasal application of 3Ro-NC has the potential to protect against transmission. Infectious SARS-CoV-2 Omicron sheds as early as 2 days before symptom onset in the upper respiratory tract. The hidden transmission link could be broken by early-stage blockage of virus entry with secretory IgA antibodies in the upper respiratory tract.

An important limitation of our study is the absence of an evaluation of viral transmission in mice or hamsters, which warrants further investigation. Our study also has several other limitations. We evaluated neither the local specific T-cell immune response, which might also contribute to the protective effect against SARS-CoV-2, nor the innate immune response in the nasal epithelium and potential local cross-variant specific T-cell immune response. Of note, the mouse model of SARS-CoV-2 Omicron infection may not be fully representative of human infection and transmission. Utilizing viral loads and infectious virus titers following challenge to assess the protective efficacy may not immunologically correlate well for assessing protection against disease due to the mild symptoms of Omicron infection in mice. In addition, the nasal vaccination regimen relies on three doses of vaccinations for full protection based on our current results obtained from mouse studies. This is indeed a disadvantage when mass vaccinations are considered for establishing herd immunity during disease emergence. However, possible self-administration adds an advantage for the nasal vaccination regimen, especially in terms of quick vaccination coverage. On the other hand, nasal vaccination with 3Ro-NC plus KFD may be used as an ideal sequential boost strategy, such as for the mass vaccination of IAV-primed vaccines. A recent study reported that a combination of systemic mRNA vaccination plus mucosal adenovirus-S immunization induced strong neutralizing antibody responses against the Omicron BA.1.1 variant [26]. The effect of 3Ro-NC plus KFD as a sequential boost strategy warrants further investigation.

Despite these limitations, our current data provide evidence that 3Ro-NC plus KFD is a unique mucosal vaccine candidate for intranasal immunization, which might provide broad protection, especially against SARS-CoV-2 Omicron infection, by inducing comprehensive local immune responses in the respiratory tract. The candidate might be a very promising mucosal vaccine that may make it possible for a safe subunit protein vaccine to be conveniently and noninvasively self-administered, which will be very useful for mass immunization during disease emergence.

MATERIALS AND METHODS

Study design

This study was designed to develop an effective mucosal subunit vaccine against SARS-CoV-2 variants of concern (VOCs), especially the Omicron variant. To assess the immunogenicity and protective efficacy of a triple RBD-based vaccine candidate, we designed a series of in vitro and in vivo

experiments. For in vivo experiments, animals were randomly assigned into groups. The sample size was determined based on previous experience and preliminary experiments by considering the variation in results and the minimum number of animals necessary for statistical analyses. All mice were included in our analysis. Sample sizes are denoted in figures or figure legends and refer to the number of animals unless stated otherwise. The antibody responses, neutralizing antibody titers, virus copies, and histopathological changes were investigated to evaluate the efficacy of the vaccines. For histological analysis, image acquisition and analysis were performed in a blinded manner.

Mice and ethics

Female 6- to 8-week-old BALB/c mice were purchased from Beijing Vital River Laboratory Animal Technology Co., Ltd., Beijing, China. HFH4-hACE2 transgenic mice on the C57BL/6 background were obtained from Dr. Ralph Baric of the University of North Carolina at Chapel Hill and bred and housed at the Animal Center of Wuhan Institute of Virology (WIV), Chinese Academy of Science (CAS). Mice were randomly assigned to groups. All mice were raised in individually ventilated cages (IVCs) under specific pathogen-free conditions. The infection experiments were performed in the Animal Biosafety Level 3 (ABSL-3) Laboratory at WIV, CAS. Animal studies were approved by the Animal Welfare and Ethical Review Committee of WIV and conducted according to Regulations for the Administration of Affairs Concerning Experimental Animals in China (study number WIVA09202101).

Vaccine preparation

The N-terminal and C-terminal regions of the D0-D1 gene of flagellin KF (*E. coli* K12 strain MG1655) were linked to construct the KFD gene, which was then cloned into the pET-28a plasmid vector (Invitrogen). The recombinant plasmid pET-28a-KFD was transformed into the *E. coli* BL21 DE3 strain and grown overnight at 37 °C in Luria–Bertani broth with 50 mg/ml kanamycin. For KFD, log-phase bacteria were induced with IPTG plus lactose, and to improve the yield of soluble protein, 1% ethanol was added 1 h before induction, and the culture temperature was reduced to 18 °C, grown for 16 h, and harvested.

The scaffold NC was designed based on the 3D structure of KFD [11] to preserve the conserved domains D0 and D1. The amino acid (aa.) identity of NC with KFD was ~72%. One RBD (aa. 319–527) of SARS-CoV-2 Omicron (B.1.1.529) variant BA.1, N region of NC, one RBD (aa. 319–527) of the Delta variant, the C region of NC and another RBD (aa. 319–527) of the Omicron variant BA.1 were sequentially linked to construct the 3Ro-NC gene. Two RBDs from the original strain (aa. 319–527) were linked to construct the RBD dimer gene. With the presence of signal peptide tPA in the 5′ region, RBDs (aa. 319–527) of the original strain, Gamma variant, Delta variant (Rd), Omicron variant BA.1 (Ro), RBD dimer and 3Ro-NC genes were cloned into the pcDNA 3.1 plasmid vector. The 293F cells obtained from Thermo Fisher Scientific were transfected with the recombinant plasmids in the presence of polyethyleneimine (PEI). Culture supernatants were harvested after growth for 72 h at 37 °C with 5% CO_2 and shaking at 130 rpm.

For each construct, a 6 × His tag or an 8 × His tag was added to the C-terminus to facilitate protein purification. The recombinant 3Ro-NC and KFD proteins were purified by affinity chromatography on a Ni-NTA column (QIAGEN), and contaminating lipopolysaccharide (LPS) was removed as previously described [15]. The residual LPS content was determined using the Limulus assay (Associates of Cape Cod) to be <0.01 EU/μg protein.

Preparation of the inactivated SARS-CoV-2 vaccine (IAV)

The inactivated vaccine was prepared as previously described [27]. Briefly, SARS-CoV-2 virus (original strain) was used to infect Vero cells. The supernatant was harvested on Day 3 or Day 4 when a cytopathic effect (CPE) was observed. Then, β-propiolactone was added to the supernatant at 1:4000 (v/v) at 2 °C–8 °C for 48 h to inactivate the virus, followed by cell debris clarification and ultrafiltration. Inactivation was validated by passaging the treated samples for three generations without the appearance of a CPE. After gel chromatography, ion-exchange chromatography, and sterile filtration, the viral particles were formulated with buffer.

Vaccination

Six- to eight-week-old female BALB/c or 12- to 16-week-old hACE2 mice were intramuscularly immunized with Imject™ Alum adjuvant (Thermo Fisher) (AL-adjuvant) in the lower hind limb or intranasally immunized with a flagellin-derived KFD protein adjuvant (KFD) three times at 3-week intervals. Intranasal immunization was performed after anesthesia with pentobarbital sodium (50 mg/kg).

Diagram of SARS-CoV-2 RBD binding with neutralizing antibodies

The crystal structures of the SARS-CoV-2 receptor-binding domain in complex with the neutralizing antibodies B38, COV2–39, CR3022 and REGN10987 were downloaded from the PDB database (PDB ID: 7BZ5, 7JMP, 6 W41, 6XDG) and imported into PyMOL. Four RBD domains were aligned together to create a 3D structure of the SARS-CoV-2 RBD bound by four different neutralizing antibodies.

Enzyme-linked immunosorbent assay

Antibody responses were assessed by enzyme-linked immunosorbent assay (ELISA). In brief, a 96-well plate was coated with the purified recombinant protein (2 μg/mL) in carbonate-bicarbonate buffer at 4 °C overnight and then blocked with 1% BSA at 37 °C for 2 h. Then, serially fourfold diluted samples were added to the plates for 2 h at 37 °C. After washing, secondary alkaline phosphatase-labeled antibodies (Goat Anti-Mouse IgG Human ads-AP antibody, or Goat Anti-Mouse IgA-AP antibody, Southern Biotech) were applied to the plates followed by substrate (p-nitrophenyl phosphate, Sigma) coloring. ODs were read at 405 nm by an ELISA plate reader (Thermo LabSystems).

Pseudotyped virus preparation and neutralization assay

To produce the SARS-CoV-2 spike pseudotyped virus, 60 μg of plasmid pNL4–3.luc. RE and 20 μg of different variants of SARS-CoV-2 spike were cotransfected with PEI into 15 cm cell culture dishes of HEK293T cells. The supernatant was harvested 72 h post transfection, centrifuged at 1000 rpm and stored at −80 °C until use. To assess the neutralizing efficiency of serum, the samples were serially diluted with DMEM supplemented with 10% FBS from 1:10 to 1:3200 in a total volume of 50 μl and then coincubated for 1 h at 37 °C with 20 μl of 200 50% tissue culture infectious doses ($TCID_{50}$) of the SARS-CoV-2 pseudotyped virus. Approximately 3×10^5 ACE2–293T cells in 30 μl of complete medium were added to each well and incubated for 48 h at 37 °C in 5% CO_2. Luciferase activity was analyzed by the luciferase assay system (Promega). The inhibition of the SARS-CoV-2 pseudotyped virus was presented as % inhibition. The 50% neutralization titers (NT_{50}) were determined by a four-parameter logistic regression using GraphPad Prism 8.0 (GraphPad Software Inc.) as previously described [16].

Antigenic cartography

The R package Racmacs (https://acorg.github.io/Racmacs/index.html) was used to create antigen cartography maps from serum neutralization titers against the SARS-CoV-2 pseudoviruses (Alpha, Beta, Gamma, Delta, Omicron BA.1 variants and the original strain Wuhan-Hu-1) and SARS-CoV-1 pseudotyped virus. Antigenic distances are measured in antigenic units (AU). One AU corresponds to a twofold dilution of the antibody in the neutralization assay. Each square in the map indicates 1 AU. The antigenic distance is measured in any direction of the map [17].

SARS-CoV-2 Omicron variant preparation and inoculation

The SARS-CoV-2 Omicron strain BA.1 (IVCAS6.7600) was provided by the National Virus Resource Center (Wuhan, China). The virus was propagated and titrated in Cercopithecus aethiops kidney cells (Vero-E6, ATCC CRL-1586). To assess the neutralizing activity of serum, the samples were serially diluted from 1:10 to 1:10240 and incubated with 200 $TCID_{50}$ of SARS-CoV-2 Omicron BA.1 at 37 °C for 0.5 h. The serum/virus volume ratio was 1:1. The mixtures were then added to Vero-E6 cells and incubated at 37 °C for an additional 1 h. The inoculum was removed, and the cells were incubated with 0.9% methylcellulose for 5 days. The 50% neutralization titers (NT_{50}) were determined by a four-parameter logistic regression using GraphPad Prism 8.0 (GraphPad Software, Inc.) as previously described [16]. For the vaccine protection experiment, 28 days after the last immunization, HFH4-hACE2 mice were intranasally inoculated with 5×10^4 $TCID_{50}$ of SARS-CoV-2 Omicron strain BA.1 in 50 μl under avertin (250 mg/kg) anesthesia. At 3 days post-infection, the mice were euthanized, and then the lung and turbinate tissues were harvested. All procedures involving infectious SARS-CoV-2 were conducted in a biosafety level-3 laboratory.

Tissue collection and virus titration

Vero-E6 cells were seeded into 24-well plates 1 day before use. Infected lungs and turbinates were homogenized in DMEM and serially diluted tenfold. The cells were inoculated with the tissue dilutions for 1 h. Next, the inoculum was removed, and the cells were incubated with 0.9% methylcellulose for 5 days. The numbers of plaques were counted after crystal violet staining to calculate the viral titer.

Histology

Lungs of mice were excised and fixed in 4% paraformaldehyde for 1 week at room temperature, followed by embedding in paraffin. After cutting into slices, tissue sections were used for hematoxylin & eosin (H&E) staining. Whole slide imaging was observed using the slide scanner Pannoramic MIDI (3DHISTECH). Pathological changes were scored on a 0–5 severity scale, as follows: 0 - normal naive parameters; 1 - slight cell infiltration and without thickened alveolar walls; 2 - moderate cell infiltration and slightly thickened alveolar walls (1–2-fold); 3 - severe cell aggregation and thickened alveolar walls (2–3-fold) in some areas; 4 and 5 - severe cell aggregation, thickened alveolar walls, blocked bronchioles and lung consolidation. Infiltration was evaluated as described elsewhere and scored on a 1–4 severity scale [28]. Scores on the inflammatory cell aggregation and interstitial pneumonia scale: 1 — normal naive parameters; 2 — slight and occasional cell aggregation; 3 — moderate cell infiltration; 4 — moderate-to-severe and multifocal cell aggregation around bronchioles or pulmonary vessels or air space of lung sections.

Statistical analysis

Means, SD, neutralizing titers and correlations were calculated using GraphPad Prism 8.0 software. A test for significance was applied as indicated in the legend of each figure. Except if otherwise indicated, statistical analysis was performed using one-way ANOVA followed by Dunnett's multiple comparison test. To analyze the differences between two groups, unpaired two-tailed Student's *t test* was used for normally distributed data with homogeneous variance, and the Mann–Whitney U test was used for nonnormally distributed data. Simple linear regression was used for correlation analysis. Analyses were performed using GraphPad Prism 8.0 software. Significance values are indicated as $^{*}P < 0.05$, $^{**}P < 0.01$, and $^{***}P < 0.001$; ns, nonsignificant. $P < 0.05$ was considered significant.

DATA AVAILABILITY

All data associated with this study are presented in the paper or the Supplementary Materials.

REFERENCES

1. Cheung PH, Chan CP, Jin DY. Lessons learned from the fifth wave of COVID-19 in Hong Kong in early 2022. Emerg Microbes Infect. 2022;11:1072–8.
2. Mannar D, Saville JW, Zhu X, Srivastava SS, Berezuk AM, Tuttle KS, et al. SARS-CoV-2 Omicron variant: Antibody evasion and cryo-EM structure of spike protein-ACE2 complex. Science 2022;375:760–4.
3. Ahn J, Kim J, Hong S, Choi S, Yang M, Ju Y, et al. Nasal ciliated cells are primary targets for SARS-CoV-2 replication in the early stage of COVID-19. J Clin Investig. 2021;131:e148517.
4. Dejnirattisai W, Huo J, Zhou D, Zahradník J, Supasa P, Liu C, et al. SARS-CoV-2 Omicron-B.1.1.529 leads to widespread escape from neutralizing antibody responses. Cell 2022;185:467–84.e15.
5. Yang J, Wang W, Chen Z, Lu S, Yang F, Bi Z, et al. A vaccine targeting the RBD of the S protein of SARS-CoV-2 induces protective immunity. Nature 2020;586:572–7.
6. Dai L, Gao GF. Viral targets for vaccines against COVID-19. Nat Rev Immunol. 2021;21:73–82.
7. Du L, He Y, Zhou Y, Liu S, Zheng BJ, Jiang S. The spike protein of SARS-CoV-a target for vaccine and therapeutic development. Nat Rev Microbiol. 2009;7:226–36.
8. WHO. https://www.who.int/publications/m/item/draft-landscape-of-covid-19-candidate-vaccines.
9. Dai L, Zheng T, Xu K, Han Y, Xu L, Huang E, et al. A Universal Design of Betacoronavirus Vaccines against COVID-19, MERS, and SARS. Cell 2020;182:722–33.e11.
10. Liu Z, Xu W, Xia S, Gu C, Wang X, Wang Q, et al. RBD-Fc-based COVID-19 vaccine candidate induces highly potent SARS-CoV-2 neutralizing antibody response. Signal Transduct Target Ther. 2020;5:282.
11. Zhao B, Yang J, He B, Li X, Yan H, Liu S, et al. A safe and effective mucosal RSV vaccine in mice consisting of RSV phosphoprotein and flagellin variant. Cell Rep. 2021;36:109401.
12. Yang J, Sun Y, Bao R, Zhou D, Yang Y, Cao Y, et al. Second-generation Flagellin-rPAc Fusion Protein, KFD2-rPAc, Shows High Protective Efficacy against Dental Caries with Low Potential Side Effects. Sci Rep. 2017;7:11191.
13. Zhong MYH, Li Y. Flagellin: a unique microbe-associated molecular pattern and a multi-faceted immunomodulator. Cell Mol Immunol. 2017;10:862–4.
14. Cao Y, Zhang E, Yang J, Yang Y, Yu J, Xiao Y, et al. Nasal epithelial GM-CSF contributes to TLR5-mediated modulation of airway dendritic cells and subsequent IgA response. J Leukoc Biol. 2017;102:575–87.
15. Yang J, Zhong M, Zhang Y, Zhang E, Sun Y, Cao Y, et al. Antigen replacement of domains D2 and D3 in flagellin promotes mucosal IgA production and attenuates flagellin-induced inflammatory response after intranasal immunization. Hum Vaccin Immunother. 2013;9:1084–92.
16. He B, Liu S, Wang Y, Xu M, Cai W, Liu J, et al. Rapid isolation and immune profiling of SARS-CoV-2 specific memory B cell in convalescent COVID-19 patients via LIBRA-seq. Signal Transduct Target Ther. 2021;6:195.
17. Lusvarghi S, Pollett SD, Neerukonda SN, Wang W, Wang R, Vassell R, et al. SARS-CoV-2 BA.1 variant is neutralized by vaccine booster-elicited serum but evades most convalescent serum and therapeutic antibodies. Sci Transl Med. 2022;14:eabn8543.
18. Lavelle EC, Ward RW. Mucosal vaccines - fortifying the frontiers. Nat Rev Immunol. 2022;22:236–50.
19. Zhu F, Zhuang C, Chu K, Zhang L, Zhao H, Huang S, et al. Safety and immunogenicity of a live-attenuated influenza virus vector-based intranasal SARS-CoV-2 vaccine in adults: randomised, double-blind, placebo-controlled, phase 1 and 2 trials. Lancet Respir Med. 2022;10:749–60.
20. Cui B, Liu X, Fang Y, Zhou P, Zhang Y, Wang Y. Flagellin as a vaccine adjuvant. Expert Rev Vaccines 2018;17:335–49.
21. He X, Chandrashekar A, Zahn R, Wegmann F, Yu J, Mercado NB, et al. Low-dose Ad26.COV2.S protection against SARS-CoV-2 challenge in rhesus macaques. Cell 2021;184:3467–73.e11.
22. Yu J, Tostanoski LH, Peter L, Mercado NB, McMahan K, Mahrokhian SH, et al. DNA vaccine protection against SARS-CoV-2 in rhesus macaques. Science 2020;369:806–11.
23. Chandrashekar A, Yu J, McMahan K, Jacob-Dolan C, Liu J, He X, et al. Vaccine protection against the SARS-CoV-2 Omicron variant in macaques. Cell 2022;185:1549–55.e11.
24. Marks M, Millat-Martinez P, Ouchi D, Roberts C, Alemany A, Corbacho-Monné M, et al. Transmission of COVID-19 in 282 clusters in Catalonia, Spain: a cohort study. Lancet Infect Dis. 2021;21:629–36.
25. Marc A, Kerioui M, Blanquart F, Bertrand J, Mitja O, Corbacho-Monne M, et al. Quantifying the relationship between SARS-CoV-2 viral load and infectiousness. Elife 2021;10:e69302.
26. Tang J, Zeng C, Cox TM, Li C, Son YM, Cheon IS, et al. Respiratory mucosal immunity against SARS-CoV-2 following mRNA vaccination. Sci Immunol. 2022:eadd4853. https://doi.org/10.1126/sciimmunol.add4853.
27. Yao YF, Wang ZJ, Jiang RD, Hu X, Zhang HJ, Zhou YW, et al. Protective Efficacy of Inactivated Vaccine against SARS-CoV-2 Infection in Mice and Non-Human Primates. Virol Sin. 2021;36:879–89.
28. Knudson CJ, Hartwig SM, Meyerholz DK, Varga SM. RSV vaccine-enhanced disease is orchestrated by the combined actions of distinct CD4 T cell subsets. PLoS Pathog. 2015;11:e1004757.

ACKNOWLEDGEMENTS

We especially thank Tao Du and Jin Xiong for their technical assistance and equipment support in the biosafety level 3 (BSL-3) facility of the Wuhan Institute of Virology, CAS. We also thank Xuefang An and Fan Zhang (core facility, Wuhan Institute of Virology, CAS) for their technical support and kind help in animal experiments.

AUTHOR CONTRIBUTIONS

HY, Z-LS, JY, and Y-QC conceptualized and supervised the study. JY, Y-QC, and ML developed the methodology. JY, LL, MX, ML, HL, XL, YH, BL, YS, and BL conducted the investigation. JY, ML, MX, and SL visualized the data. JY, HY, Y-QC, and Z-LS wrote the original draft. All authors reviewed and edited the paper.

FUNDING

This work was supported in whole or in part by the National Key R&D Program of China (grant number: 2021YFC2302602 to JY), the strategic priority research program (grant number XDB29010101) and key project (2020YJFK-Z-0149) of the Chinese Academy of Sciences (to Z-LS). This study was also supported by the National Natural Science Foundation of China (31970878 to JY, 92169104 and 31970881 to Y-QC), Shenzhen

Science and Technology Program (Grant number: RCJC20210706092009004 and JCYJ20190807154603596 to Y-QC).

COMPETING INTERESTS

The authors declare no competing interests.

ADDITIONAL INFORMATION

Supplementary information The online version contains supplementary material available at https://doi.org/10.1038/s41423-022-00929-3.

Correspondence and requests for materials should be addressed to Yao-Qing Chen, Zheng-Li Shi or Huimin Yan.

Reprints and permission information is available at http://www.nature.com/reprints

Springer Nature or its licensor holds exclusive rights to this article under a publishing agreement with the author(s) or other rightsholder(s); author self-archiving of the accepted manuscript version of this article is solely governed by the terms of such publishing agreement and applicable law.